

# Laser induced structure transformation in $\text{Co}_{70}\text{Fe}_3\text{Mn}_{3.5}\text{Mo}_{1.5}\text{B}_{11}\text{Si}_{11}$ amorphous alloy

STEPAN I. MUDRY, YULIA S. NYKYRUY\*

Ivan Franko Lviv National University, Physics of Metals Department, Kyrylo and Mephodyj str., 8, Lviv 79005 Ukraine

Laser induced structure changes in amorphous  $\text{Co}_{70}\text{Fe}_3\text{Mn}_{3.5}\text{Mo}_{1.5}\text{B}_{11}\text{Si}_{11}$  alloy have been studied by means of X-ray diffraction and magnetic properties measurements. Both three types of structural relaxations and a starting stage of crystallization process are considered as main characteristics of structure transformation upon laser treatment. Results of investigation of this amorphous alloy at different parameters of laser irradiation have shown that this alloy becomes partly crystalline after irradiation with laser pulse fluence of about  $1.8 \text{ J/mm}^2$  and pulse duration  $\tau = 2 \times 10^{-5} \text{ sec}$ . Increasing of laser pulse fluence above  $2.0 \text{ J/mm}^2$  leads to the destruction of ribbon, due to intensive evaporation.

Keywords: *amorphous alloy; relaxation and crystallization processes; laser irradiation*

© Wrocław University of Technology.

## 1. Introduction

During last few decades amorphous metallic alloys have attracted the attention of researchers owing to their unique properties, which permitted using those materials in various areas of industry. A major feature of amorphous alloys, making them different from the crystalline ones, is the lack of long-range order in atomic arrangement. Thus, they have only short-range order structure, which determines the most of physical and chemical properties (mechanical, electrical, magnetic, etc.).

In order to improve the properties of amorphous alloys, which are responsible for their application, various methods are commonly employed and one of them – thermal treatment is most widely used. Over last few years by means of this method, a lot of nanocrystalline and amorphous composites with improved properties have been produced. Less attention was paid to laser treatment of amorphous alloys. Available are only few works, in which the influence of laser irradiation on the structure and physical properties of amorphous metallic alloys are studied, most of which are devoted to Fe-based [1–5] and some to Co-

based alloys [6–8]. The aim of this work is to study the change of structure after laser irradiation of  $\text{Co}_{70}\text{Fe}_3\text{Mn}_{3.5}\text{Mo}_{1.5}\text{B}_{11}\text{Si}_{11}$  amorphous alloy.

## 2. Experimental

Amorphous  $\text{Co}_{70}\text{Fe}_3\text{Mn}_{3.5}\text{Mo}_{1.5}\text{B}_{11}\text{Si}_{11}$  alloy was prepared by spinning method and the thickness of obtained ribbons was about  $25 \mu\text{m}$  and the width of  $0.020 \text{ m}$ .

Laser treatment has been carried out using Laser Graver equipment (Alpha R&M, Russia). Wavelength of laser radiation  $\lambda$  was equal to  $1.06 \mu\text{m}$ ; pulse frequency,  $f = 50 \text{ kHz}$ ; pulse duration,  $\tau = 2 \times 10^{-5} \text{ s}$ ; scanning step =  $20 \mu\text{m}$ ; laser pulse fluence,  $Q = 1.15 - 2.0 \text{ J/mm}^2$ .

Features of structural transformations of irradiated samples were studied by X-ray diffraction method (Fe- $K\alpha$  radiation,  $\lambda = 1.9373 \text{ \AA}$ ). Scattered intensities obtained at various angles of diffraction were corrected by polarization and absorption factors taking incoherent scattering into account. The corrected intensity values were used in this procedure to calculate the structure factors (SF). Pair correlation functions (PCF) were calculated from the SF's using the integral Fourier transformation. The first peak position of this function

\*E-mail: k-nik-julia@yandex.ru

has been interpreted as the most probable inter-atomic distance  $r_1$  [9].

For the analysis of the structural changes, the experimental diffraction peak has been reproduced by means of approximation by Lorentz function using a program Origin 6.1. The volume fraction of the nanocrystalline phase  $X_{cr}$  was calculated using the relation [10]:

$$X_{cr} = I_{cr} / (I_{cr} + I_{am}) \quad (1)$$

where  $I_{am}$  and  $I_{cr}$  are total intensities of the maxima for amorphous and nanocrystalline phases, respectively.

Cluster size  $L$  has been calculated using formula  $L = 2\pi/\Delta s$ , where  $\Delta s$  – is half-peak width. Certainly, the width of the diffraction peak, which is used for determination of clusters size, is related also with internal stresses. However, the influence of the stresses on the diffraction pattern is proportional to  $\tan\theta$  ( $\theta$  – half of scattering angle) and is not large enough for principal peak. For that reason, the influence of inner stresses on determination of structural units size was neglected in this work.

The temperature dependence of the saturation magnetization in a field of 800 kA/m was measured using a vibrating magnetometer. Heating and cooling was carried out at a rate of 30 K/min in the temperature range of 300 K to 1000 K. These dependences were used to estimate the Curie temperature ( $T_C$ ) of the amorphous and crystalline phases and crystallization temperature ( $T_x$ ).

### 3. Results and discussions

It is clear that laser irradiation induces the high speed heating of ribbon surface in local area and such local heating results in structural transformations which depend on laser fluence. Structural changes for the alloy under investigation can be observed in X-ray diffraction (XRD) patterns (Fig. 1), which have been obtained for different laser pulse fluences.

As is seen, the principal peaks of the intensity curves at fluence values within an interval of 0 – 1.4 J/mm<sup>2</sup> reveal a typical amorphous structure whose parameters depend on the laser pulse fluence. At low fluence values this peak shows a

symmetrical profile, but it should be noted that it becomes narrower and its height increases with the fluence increasing. Such behavior is an evidence of topologic ordering increase, which is supposed to be caused by atomic rearrangement due to diffusion process as well as free volume decrease. Besides, the decrease of half-peak width is also observed indicating the increase of the size of zones of the coherent scattering, which are commonly observed as clusters. Therefore, we consider the cluster as a correlated group of atoms, which has some structural ordering in atomic distribution, but atoms in the clusters can change their positions more easily in comparison to the ones in crystalline grains.

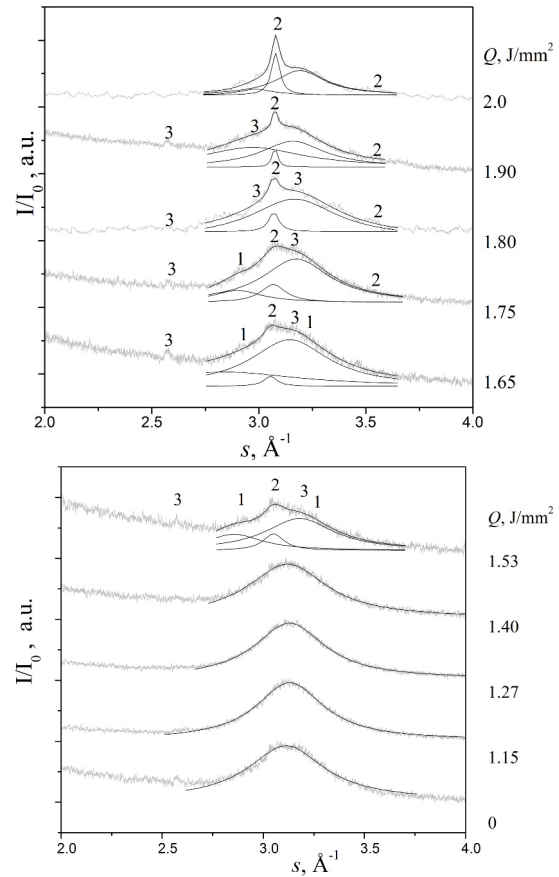


Fig. 1. Diffraction patterns of amorphous alloy at different pulse fluences compared with peak positions of crystalline phases of –  $\alpha$ -Co (1);  $\beta$ -Co (2);  $\text{Co}_3\text{B}$  (3).

At higher values of laser fluence (about 1.5 J/mm<sup>2</sup>) the asymmetry and then the splitting of

principal maximum occurs. All this is supposed to be caused by formation of more complex structure, consisting of two or more kinds of clusters. Moreover, the patterns that correspond to fluence values within  $1.5 - 1.8 \text{ J/mm}^2$  range show the small crystalline like peaks. Identification of these peaks has shown, that they are close to diffraction maxima for  $\alpha$ -Co,  $\beta$ -Co and  $\text{Co}_3\text{B}$  crystalline phases, which usually crystallize during isothermal annealing of amorphous alloys in Co-Si-B system [11, 12]. So, at the laser fluence of about  $1.5 \text{ J/mm}^2$  the formation of clusters with the structure similar to the structure of mentioned crystalline phases occurs. Certainly, such clusters cannot reach the critical size to transform itself into stable nucleation centers, from which at suitable thermodynamic and kinetic conditions the formation of nanocrystals occurs. Therefore, the formation of clusters with another structure than the structure of amorphous matrix is caused by laser irradiation and this process can be considered as pre-crystallization process [13]. At more intensive laser pulse fluence ( $Q > 1.75 \text{ J/mm}^2$ ) the peak, which is close to diffraction maxima for  $\beta$ -Co phase rises up with fluence increasing. Since the principal peak positions for  $\alpha$ -Co and  $\beta$ -Co – phases are close to each other we have analyzed the next peaks in diffraction patterns, particularly more separated from the second peaks that allowed us to conclude the formation of  $\beta$ -Co phase.

It is clear that the structure changes following from the analysis of diffraction patterns, should be accompanied by variation of such parameter as most probable interatomic distance. This parameter for amorphous phase (Fig. 2a) decreases with increasing the pulse fluence, but at low fluences this decrease is notably less than at higher fluence values. The observed behavior allowed us to suggest that small decreasing of  $r_1$  is related to volume reduction at relaxation, whereas a more drastic decreasing occurs due to formation of more ordered atomic distribution. Such structure transformation at low fluences, according to Egami classification [14], can be attributed to structural changes of the first type, at which the distance between the nearest neighbors decreases, whereas the structure changes at higher fluence values can be attributed

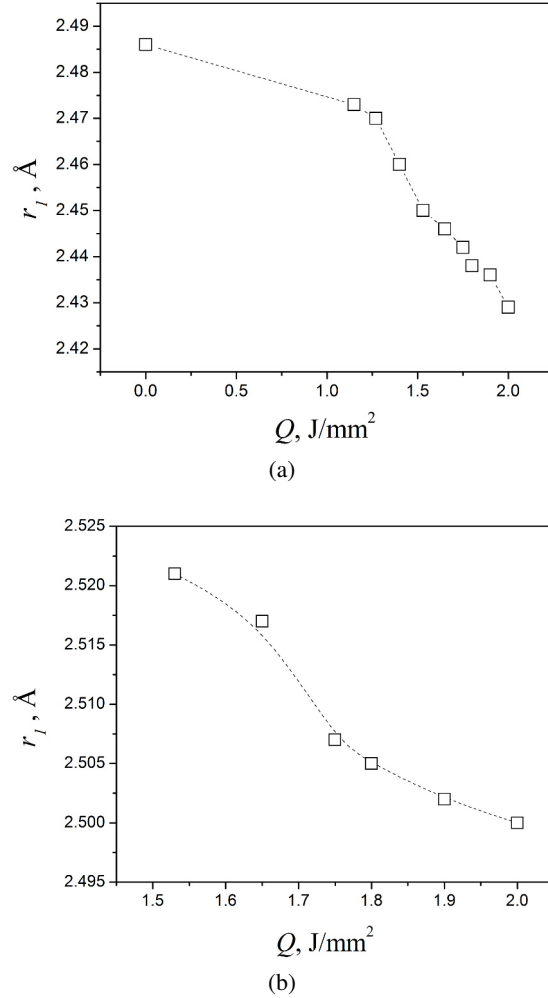


Fig. 2. Most probable interatomic distance versus laser fluence for amorphous matrix (a) and  $\beta$ -Co clusters (b).

to structural changes of the second type – forming topological short-range order, at which the formation of small crystalline clusters occurs [15].

At pulse fluence  $Q = 1.7 - 1.9 \text{ J/mm}^2$  an interatomic distance  $r_1$  of already formed clusters rapidly decreases (Fig. 2b). This process can be attributed to the third type of structural changes at which, according to Chen [16], phase separation and chemical short-range order are forming. It is suggested [3] that the processes corresponding to the 2 and 3 types precede the crystallization process.

At higher fluence values ( $Q = 1.9 - 2.0 \text{ J/mm}^2$ ) parameter  $r_1$  for crystalline clusters becomes closer to such parameter of crystalline  $\beta$ -Co ( $2.506 \text{ Å}$ ).

It is clear that transition from a cluster structure to nanocrystalline one is accompanied by cluster size increase. To nowadays the critical size of clusters, when the transition from clusters to nanocrystals occurs, has not been determined definitely. According to [17] the characteristic feature of this transition at increasing of cluster size is an appearance of symmetry in atomic distribution in nanocrystals. Such symmetry can be revealed by detailed analysis of diffraction patterns. In case of cluster structure, we observe only one diffraction peak, whereas in case of nanocrystals more peaks should be pronounced. For that reason, we have carried out the detailed analysis of diffraction patterns in the vicinity of the first and second maxima for crystalline  $\beta$ -Co (Fig. 3).

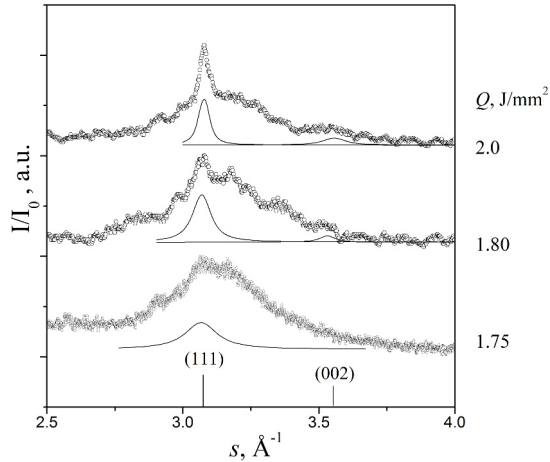


Fig. 3. Analysis of the first and second maxima in diffraction patterns for crystalline  $\beta$ -Co.

Cluster size versus laser pulse fluence of amorphous and  $\beta$ -Co phases (Fig. 5) is in accordance with the analysis of second maxima in diffraction patterns. As can be seen from Fig. 5, cluster size  $L$  of amorphous phase increases with fluence increasing and its maximum value is 1.7 nm at a fluence about 1.3  $\text{J}/\text{mm}^2$ . With further fluence increasing the cluster size decreases, which is supposed to be caused by degradation of amorphous phase. Another dependence is observed for crystalline clusters, which reveal the increase over all fluence values. Therefore, for crystalline like structures we have opposite tendency – the transition from small cluster with slight topologic ordering to the larger

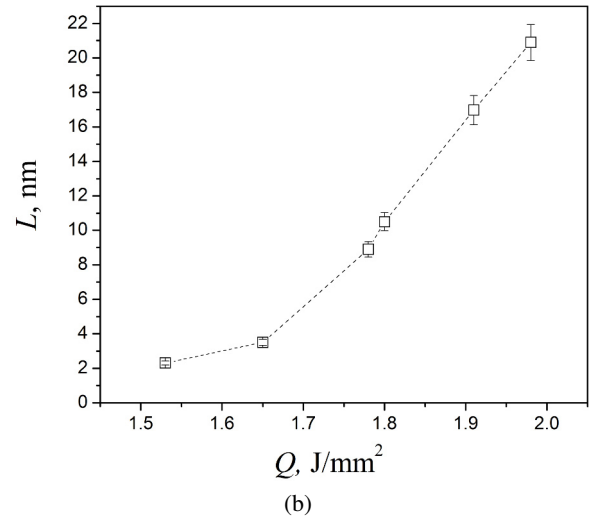
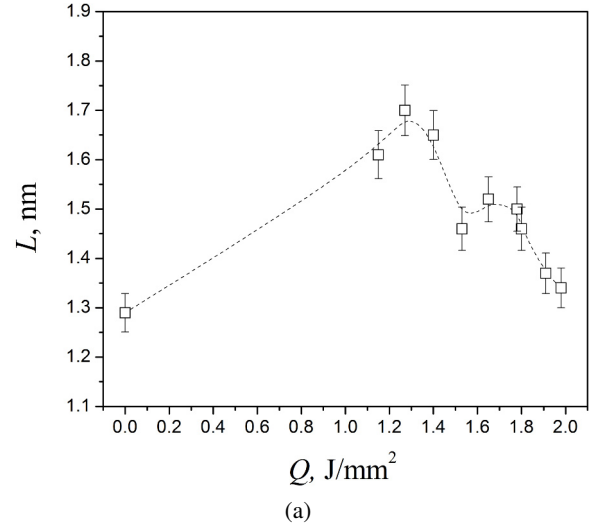


Fig. 5. Cluster size versus laser pulse fluence for amorphous (a) and  $\beta$ -Co (b) phases.

ones with  $\beta$ -Co atomic distribution phase. As an origin of crystalline phase is the emergence of critical nuclei, their size can be considered as the lower limit of the nanocrystalline state, i.e., as the smallest possible size of nanocrystals that can be formed by crystallization [18]. According to [17], the critical size  $L_{cr}$  of the crystal is the size at which it still retains the all inherent to this type of crystal elements of symmetry, and which, in the framework of this approach, is equal to three coordination spheres. Thus, using the value of  $r_1$ , the critical size of the nucleus of the crystalline phase of  $\beta$ -Co has been determined as  $L_{cr} \sim 7.5 \text{ \AA}$ . Since

$L$  of  $\beta$ -Co phase within the entire fluence values (Fig. 4b) exceeds  $L_{cr}$ , this phase can be considered as nanocrystalline, and the process of its formation as the beginning of crystallization.

The fraction of nanocrystalline  $\beta$ -Co phase rises up to  $\sim 12\%$  at  $Q = 2.0 \text{ J/mm}^2$ . At laser pulse fluence larger than  $Q = 2.0 \text{ J/mm}^2$  intensive melting and vaporization occurs that results in alloy destruction. Therefore, it is difficult to complete the crystallization process with this kind of laser treatment. This can be due to short time of heating, caused by short pulse duration, and high speed of cooling that is inherent for laser processing.

It is known that structure changes are associated with changes of many physical properties. For Co-based alloys the magnetic properties are such the ones that significantly depend both on atomic and nanoscale structure. We suggest that structure changes upon laser treatment can be used to improve also the magnetic properties. In order to verify this suggestion a magnetization as a function of temperature has been measured. Amorphous  $\text{Co}_{70}\text{Fe}_3\text{Mn}_{3.5}\text{Mo}_{1.5}\text{B}_{11}\text{Si}_{11}$  alloy was heated to the temperature of 1000 K with a rate of 30 K/s and then cooled with the same rate.

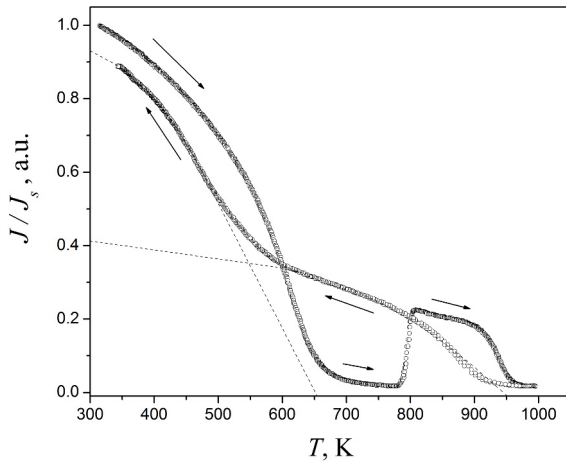


Fig. 6. Magnetization versus temperature.

Magnetization along with the rise in temperature is diminishing monotonically achieving the Curie point ( $T_C$ ) at temperature of 635 K, and then shows the drastic increase at 788 K that is due to the start of crystallization process (Fig. 6). In con-

trast to magnetization versus temperature curve for alloys of Co-Si-B [19, 20], and Co-Fe-Mo-Si-B systems [21], the obtained curve reveals a wide paramagnetic region. The comparison of data reported in [19, 20] and [21] with those, presented in Fig. 6, displays that addition of Fe and Mo to Co-Si-B alloy results in Curie temperature reducing, moreover, addition of Mn to Co-Fe-Mo-Si-B results in further reduction of Curie temperature but increase of the temperature at which the crystallization process starts. The obtained value of  $T_C$  for  $\text{Co}_{70}\text{Fe}_3\text{Mn}_{3.5}\text{Mo}_{1.5}\text{B}_{11}\text{Si}_{11}$  amorphous alloy is in well agreement with the value obtained in [22] (638 K). The temperature at which crystallization starts for investigated alloy is close to the value obtained by DTA method for similar  $\text{Co}_{71.5}\text{Fe}_{2.5}\text{Mn}_2\text{Mo}_1\text{Si}_9\text{B}_{14}$  alloy (789 K) [23].

Curie temperature for crystalline phases ( $T_C^{cr}$ ), obtained from thermo-magnetic curve is about 950 K. As it was noted above, phases that usually crystallize during heating in Co-based alloys are  $\alpha$ -Co,  $\beta$ -Co and  $\text{Co}_3\text{B}$ . Nevertheless, in [24] it was reported the formation of  $\alpha$ -Fe and  $\text{Co}_3\text{Mo}$  phases as well as small amount of  $\text{Co}_2\text{Mo}_3$  [25]. As for  $\beta$ -Co,  $\text{Co}_3\text{B}$ , and  $\alpha$ -Fe phases, their Curie temperatures are 1400 K, 747 K, 1044 K, respectively [26]. These values are different from the value of 950 K, obtained in this work. Such discrepancy can be caused by various reasons, but most probably it is due to formation of different magnetic phases, both an amorphous and crystalline ones.

Next cooling at the same rate results in increasing of magnetization, which is the proof of crystallization of the phase with magnetic properties. As displayed in Fig. 6, the magnetization value during cooling in temperature range below 500 K is lower than the corresponding value during heating. Similar behavior was also observed for  $\text{Co}_{68}\text{Fe}_4\text{Mo}_1\text{Si}_{13.5}\text{B}_{13.5}$  [21].

It should be noted that the magnetization versus temperature that is observed at cooling, is characterized by two inflection points. Most probably, such behaviour is caused by the formation of two or more magnetic phases upon crystallization. Certainly, the magnetic characteristics of such phases are different and for one of them, the Curie temperature can be approximately estimated by means of



fitting of two partial curves of magnetization to the experimental one, as it is shown in Fig. 6.

Therefore, the significant dependence of magnetic properties of  $\text{Co}_{70}\text{Fe}_3\text{Mn}_{3.5}\text{Mo}_{1.5}\text{B}_{11}\text{Si}_{11}$  amorphous alloy on temperature, observed at conditions, which are close both to equilibrium heating and cooling, allowed us to suggest that in the conditions far from equilibrium such dependence may also occur, offering the way to obtain magnetic materials with improved properties.

## 4. Conclusions

The process of laser-induced structural transformation of amorphous  $\text{Co}_{70}\text{Fe}_3\text{Mn}_{3.5}\text{Mo}_{1.5}\text{B}_{11}\text{Si}_{11}$  alloy was investigated. Three types of structural transformations that correspond to the process of reducing the free volume, topological and chemical ordering have been observed. At the early stage of structure changes the clusters with a structure similar to the  $\text{Co}_3\text{B}$ ,  $\alpha\text{-Co}$  and  $\beta\text{-Co}$  phase are formed, but only  $\beta\text{-Co}$  becomes a stable nucleus at higher values of laser pulse fluence. The fraction of  $\beta\text{-Co}$  nanocrystals in amorphous matrix rises up proportionally to fluence within the interval of 1.75 – 2.0 J/mm<sup>2</sup>, achieving 12 %, and the crystal size rises up to ~22 nm. Further increase of fluence leads to destruction of the ribbon due to evaporation.

High sensitivity of magnetization to temperature permits using laser irradiation for optimization of magnetic properties.

## References

- [1] JALEH B., VALIEGHBAL M., HABIBI S., TORKAMANY M.J., *J. Supercond. Nov. Magn.*, 25 (2012), 2665.
- [2] ZELENAKOVA A., KOLLAR P., VERTESY Z., KUZMINSKI M., RAMIN D., RIEHEMANN W., *Acta Phys. Slovaca*, 50 (4), (2000), 501.
- [3] GIRZHON V.V., SMOLYAKOV A.V., BABICH N. G., SEMEN'KO M.P., *Phys. Met. Metallogr.*, 108 (2) (2009), 125.
- [4] LYASOTSKYI I.V., DYAKONOVA N.B., DYAKONOV D.L., KRAPOSHIN V.S., *JPCS*, 98 (2008), 120.
- [5] LANOTTE L., IANNOTTI V., *J. Appl. Phys.*, 78 (5) (1995), 3531.
- [6] FEDOROV V.A., JAKOVLEV A.V., KAPUSTIN A.N., VASILEVA I.V., *Rev. Adv. Mater. Sci.*, 20 (2009), 179.
- [7] KRAVETS V.G., PORTIER X., PETFORD-LONG A.K., *J. Mater. Sci.*, 37(13) (2002), 2773.
- [8] GIRZHON V.V., RUDNEV YU.V., ANPILOGOV D.I. AND SMOLYAKOV A.V., *Scripta Mater.*, 39 (6) (1998), 815.
- [9] YOSHIO WASEDA, *The structure of non-crystalline materials. Liquids and amorphous solids*, McGraw-Hill International Book Co., New York, 1980.
- [10] SESTAK J., MARES J., HUBIK P. (Eds.), *Glassy, Amorphous and Nano-Crystalline Materials: Thermal Physics, Analysis, Structure and Properties*, Springer Science+Business Media B.V., New York, 2011.
- [11] LESZ S., NOWOSIELSKI R., ZAJDEL A., KOSTRUBIEC B. AND STOKŁOSA Z., *Arch. Mater. Sci. Eng.*, 28 (2) (2007), 91.
- [12] MUDRY S., KOTUR B., BEDNARSKA L., KULYK YU., *J. Alloy. Compd.*, 367 (2004), 274.
- [13] SUZUKI K., FUJIMORI H., HASHIMOTO K. (Eds.), *Amorphous Metals. Metallurgy*, Moscow, 1987 (in Russian).
- [14] EGAMI T., *Mater. Res. Bull.*, 13 (1978), 557.
- [15] MASUMOTO T., MADDIN R., *Mater. Sci. Eng.*, 19 (1975), 1.
- [16] CHEN H. S., *Rep. Prog. Phys.*, 43 (1980), 432.
- [17] GLEZER A.M., *Ros. Khim. Zh. (Zh. Ross. Khim. Ob-va im. D.I. Mendeleeva)* XLVI (5) (2002), 57, (in Russian).
- [18] ANISHCHIK V.M., BORISENKO V.E., ZHDANOK S. A., TOLOCHKO N. K., FEDOSYUK V. M. (Eds.), *Nanomaterials and nanotechnologies. Izd. Center BSU*, Minsk, 2008, (in Russian).
- [19] NOWOSIELSKI R., ZAJDEL A., LESZ S., KOSTRUBIEC B., STOKŁOSA Z., *JAMME*, 17 (1 – 2) (2006), 121 – 124.
- [20] LESZ S., NOWOSIELSKI R., KOSTRUBIEC B., STOKŁOSA Z., *JAMME*, 16 (1 – 2) (2006), 35.
- [21] KONIECZNY J., BORISJUK A., PASHECHKO M., DOBRZANSKI L.A., *JAMME*, 42 (1 – 2), (2010), 42.
- [22] *VITROPERM 500 F – VITROVAC 6030 F. Tape-wound cores for power transformers in SMPS*, Vacuum-schmelze GmbH & Co. Hanau, Germany
- [23] JAKUBCZYK E., KOLANO R., *Visnyk Lviv Univ. Ser. Physic.*, 33 (2000), 233.
- [24] HE SHU-LI, HE KAI-YUAN, WANG ZHI, CHENG LI-ZH, FU YU-JU., *Chinese Phys. Lett.*, 14 (6) (1997), 464.
- [25] LACHOWICZ H.K., POPLAWSKI F., ZUBEREK R., KUTMIDSKI M., QLAWSKA-WANIEWSKA A., DYNOWSKA E., *IEEE Magn.*, 35 (5) (1999), 3877.
- [26] GRIGOR'EV I.S., MEILIKHOV E.Z. (Eds.), *Fizicheskie velichiny: Spravochnik (Handbook of Physical Quantities)*, Energoatomizdat, Moscow, 1991.

Received 2013-09-11

Accepted 2013-12-02